# CTF APPLICATION TO BWR MODELING AND SIMULATIONS

**C. Gosdin[1], M. Avramova[1] and R. Salko[2]**
[1] Department of Mechanical and Nuclear Engineering, Pennsylvania State University,
231 Reber Building, University Park, PA 16802, USA
[2]: Oak Ridge National Laboratory, Oak Ridge, TN 37831, USA
cag5281@psu.edu, mna109@psu.edu, salkork@ornl.gov

**ABSTRACT**

CTF, the version of COBRA-TF being jointly developed and maintained by Pennsylvania State University and Oak Ridge National Laboratory for applications in the Consortium for Advanced Simulation of Light Water Reactors (CASL), uses a two-fluid, three-field representation of two-phase flow, which makes it capable of modeling the high-void flow expected in BWR operation. This paper focuses on application of CTF to mini- and whole-core BWR calculations on the pin-cell resolved level as well as demonstrating that CTF can properly model bypass flow. To increase the confidence in CTF's BWR modeling capabilities, extensive simulations have been performed using the international Organization for Economic Cooperation and Development (OECD) / US Nuclear Regulatory Commission (NRC) Oskarshamn-2 benchmark, including modeling of a single and 2x2 assemblies on pin by pin level, and a full core model on assembly level. Each model is varied, with an increasing amount of detail. The results demonstrate that CTF is capable of modeling basic and complex BWR simulations. Using the three Oskarshamn-2 simulations, CTF's capabilities of modeling BWRs was further verified.

**KEYWORDS**
BWR, CTF, CASL, Subchannel, Validation

## 1. INTRODUCTION

COBRA-TF is a best-estimate thermal-hydraulic subchannel code that was originally developed by the Pacific Northwest National Laboratory in 1980 [1]. CTF is an improved version of COBRA-TF that has been maintained and further developed by the Reactor Dynamics and Fuel Management Group (RDFMG) at the Pennsylvania State University (PSU). This version of the code is currently being jointly improved, maintained, and tested by PSU and Oak Ridge National Laboratory for applications in the US Department of Energy (DOE) program Consortium for Advanced Simulation of Light Water Reactors (CASL). The code provides a three-dimensional, two-fluid, three-field representation of two-phase flow, the liquid phase is subdivided into a continuous field and an entrained liquid drop field. Therefore, CTF solves three momentum conservation equations, three mass conservation equations, and two energy conservation equations [2]. A thermal equilibrium is assumed between the continuous liquid field and the droplet field [3], leading to a set of eight equations solved for the fluid portion. The code also includes conduction equations with special models for nuclear fuel rods, allowing for coupled fluid/solid solutions.

There are currently specific versions of COBRA-TF, such as F-COBRA-TF (AREVA NP copyrights) that have been recently validated for BWR applications. Both CTF and F-COBRA-TF originate from the same Penn State version of COBRA-TF from the 1990s [4]. Since then, a large amount of in-house development was done to the point where F-COBRA-TF has been verified and validated and used for both types of LWRs [5]. The code was validated using the OECD/NRC Boiling Water Reactor Full-length Bundle Test (BFBT) benchmark and AREVA-NP in-house measurements.

The ability to correctly predict pressure losses in two phase-flow is vital to modeling of BWRs. This includes effects from wall drag, interfacial drag, and form losses due to the presence of spacer grids. CTF includes a two-phase pressure drop model based on the work of Wallis and grids are treated using simple velocity head losses [6]. Spacer grids also have an impact on rod heat transfer due to enhanced turbulence and boundary layer disruption within and downstream of the grid [7]. In very high void conditions, entrained droplets are broken up into smaller drops, which increases the droplet surface area and interfacial heat transfer. Additionally, rewetting of the spacer grid in accident conditions leads to cooling of the superheated vapor flowing through the core [8]. An analysis of steady state and transient void distribution predictions for Phase I of the OECD/NRC BFBT benchmark using CTF/NEM [9]. The CTF validation to the OECD/NRC BFBT benchmark single- and two-phase pressure drop exercises has proven the code capabilities of predicting pressure losses in a BWR environment [10].

This paper discusses the results obtained from three different BWR CTF models: single assembly on pin-cell resolved level (model 1), 2x2 array on pin-cell resolved level (model 2), and full core on assembly-cell resolved level (model 3). Each model had three levels of detail that investigated effects of internal flow, external flow, and flow inside water rods. All tests were modeled at steady state conditions and follow the Oskarshamn-2 specifications [11].

## 2. CTF MODELS

The three models discussed are presented in Table 1 along with the operating conditions. Table 2 shows the variation in detail that each model has undergone. Internal bypass was defined as a bypass region between assemblies, while external bypass was defined as a bypass region that surrounds the assembly (see Figures 3 and 4). The water channel was defined as a bypass region that is located at the center of the assembly. This acts similar to a water rod, but is inherently a bypass region. Finally table 3 lists all assumptions used for each model.

**Table 1: Operating Conditions**

| | Pressure (bar) | Linear Heat Rate (kw/m) | Assemblies | Resolution | Partial Rod |
|---|---|---|---|---|---|
| Model 1 | 70.2 | 14.8946 | 1 | Pin-cell level | Two sections |
| Model 2 | 70.2 | 14.8946 | 4 | Pin-cell level | Geometry variation |
| Model 3 | 71.66 | 15.8319 | 444 | Assembly-cell level | Two sections |

**Table 2: Model Variation**

| | Internal bypass | External bypass | Water channel bypass |
|---|---|---|---|
| Base case | Not included | Not included | Not included |
| Bypass case | Included | Included | Not included |
| Water Channel | Included | Included | Included |

**Table 3: Model Assumptions**

| | |
|---|---|
| **General Assumptions [12]** | |
| 1. | The corners of the assembly in Figure 1 are square in the model. This is due to insufficient information given including the radius of curvature for the corners. As a result, it is expected to increase the flow area of the corner subchannel increasing the flow and reducing the void generation with the same bundle flow conditions. |
| 2. | The default material properties for $UO_2$ in CTF are used instead of the properties in the specifications. The reason for this assumption is convergence issues when pre-specified properties are used - one noticeable difference is the thermal conductivity, which differs by a large amount. These properties were taken from MATPRO-11 [13]. |
| 3. | The assembly boxes are modeled using the same material as the fuel cladding. This assumption is made due to no information on the actual material referenced in the specifications. This assumption should not affect the models by any substantial amount since most boxes are made from similar material as the cladding; and when steady state conditions are assumed |
| 4. | The external bypass realistically would contain objects protruding from the walls of the adjacent tanks, acting as structural supports. These supports are not modeled in the area. |
| 5. | A constant gap conductance of 11356.0 btu/(h ft$^2$ $^o$F) was used. A constant radial power distribution in the fuel pellet was used. |
| 6. | Plenums are not being modeled, meaning the bypass regions do not connect at the top and bottom of the assemblies. |
| **Full Core Assumptions [12]** | |
| 7. | All transverse gaps between subchannels are removed from the model inputs. This simplification is needed to reduce the complexity of the model allowing it to converge. This should not cause any substantial effects due to the assumed small amount of flow between the internal bypass channels and small temperature gradients. |
| 8. | The dimensions for water rods in Type 1 assemblies are not given in the specifications, as a result approximations were taken from a previous model at PSU. |

## 2.1. Single Assembly on a Pin-Cell Resolved Level

The first and simplest model was a single assembly consisting of 91 fuel rods (8 partial and 83 full rods), shown in Figure 1. The rods colored red indicate a partial rod, which is a fuel rod that is not the full rod length. Figure 4 below shows the difference between the rod types, these are used as a way of controlling the reactor. An ATRIUM-10 assembly from the Oskarshamn-2 specification was used for all input values [6]. The model had three variations, shown below in Figure 2. The initial model consisted of just the assembly, with the area the water rod acting as a solid adiabatic surface. Each subsequent variation added detail to the previous. The first addition was a bypass that surrounds the assembly. The next addition was a water rod, which was modeled as a water channel bypass, at roughly the center of the assembly that took the place of 9 fuel rods.

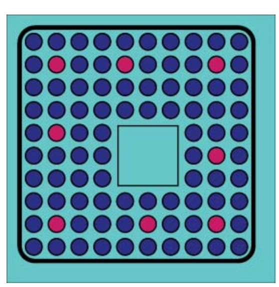

**Figure 1: Single BWR assembly pattern**

CTF was able to model partial rods in two different structures. Since BWRs typically contain partial rods that are paramount to the design, it was important simulations are created to model them as close to realistically possible. This single ATRIUM-10 assembly model had two axial sections: one containing all 91 rods, and the second upper section containing only the tops of the full length rods.

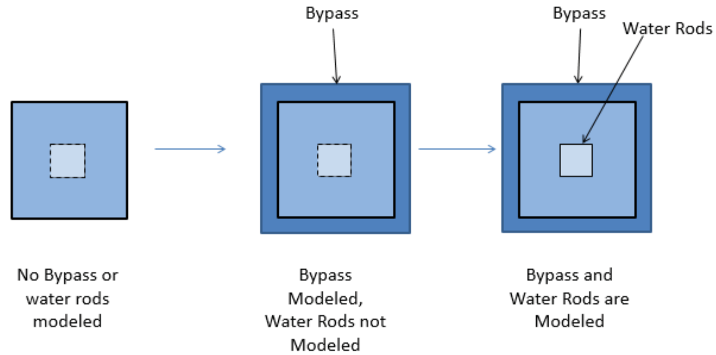


**Figure 2: Varying models of complexity for single BWR assembly**

2.2. 2x2 Array Assemblies on Pin-cell Resolved Level

The second model was an expansion of the previous model. The single assembly was expanded into a 2x2 array following the same path of detail as shown below in Figure 3. Since the model contained multiple assemblies, the bypass was split up into internal and external sections. Each bypass section was created the same way as was done for the single assembly case. However, instead of splitting the rods into two axial sections, the partial length rods were captured using the axial geometry variation feature. By changing the size of the channels and gaps around the partial rods at a specific height (in this case the point at which they end), it effectively creates a new area without splitting the rods into two sections. The expansion modeling can be seen in Figure 4, note that this method will show little change in the overall pressure loss, but local flow and enthalpy distributions may be slightly different. Graphics in Figure 4 depict the two different possible modeling techniques used for this simulation.

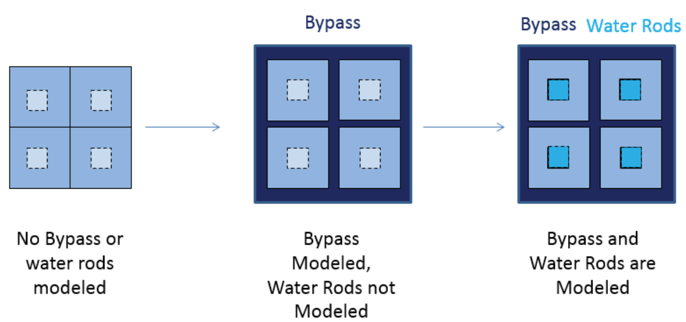


**Figure 3: Varying models of complexity for 2x2 BWR array**

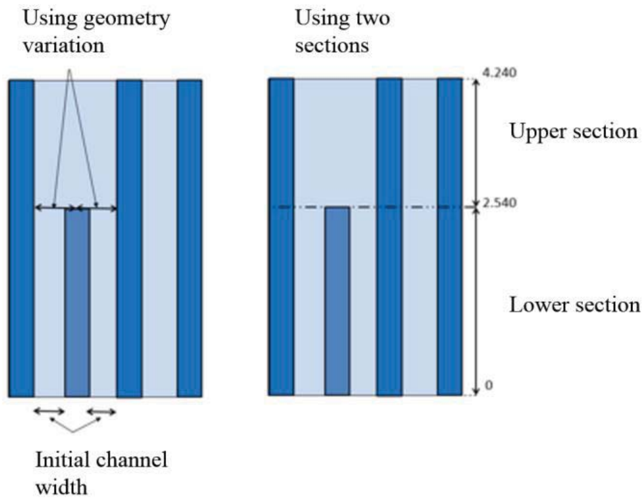


**Figure 4: Possible modeling schemes for CTF**

2.3. Full Core on Assembly-Cell Resolved Level

The last model represents the core on an assembly-level rather than pin-by-pin. Therefore the fuel pins for each assembly were modeled as one single channel, meaning each assembly simulated one single lumped fuel rod with the flow through the entire assembly represented as a single channel. The last model was originally developed within the European Community NURESAFE project [11] and was subsequently updated by PSU [12]. There were 470 assemblies consisting of 4 different assembly types in the input, which are shown in Figure 5. The difference between assembly types 2 and 3 was the loss coefficient in the spacers.

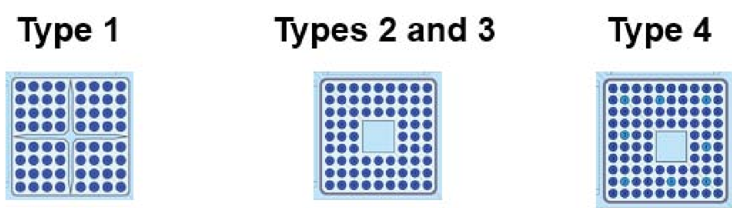


**Figure 5: Full core assembly types [12]**

The full core model followed the same trend as the previous decks of increasing detail. The first model was a basic model that does not model either water rods or bypass regions of the core. The second model has both internal and external bypass regions of the core. The last model takes the model 2 design and adds in water rods as another level of detail. The water rods in each assembly have Zircaloy cladding surrounding them and are a different size and shape for each assembly type.

## 3. RESULTS

Each case was run until completion using the CTF internal pseudo-steady-state convergence criteria that checks engineering parameters of interest, including fluid and solid energy balance and storage. Each model was then analyzed by examining the following in bundle channel fluid properties for each variation: pressure and vapor void fraction. For models 1 and 2, channel 39 was analyzed, located next to the water channel. For the full core, three different channels, were analyzed, one for each type of different assembly. It was also significant to look at the similarities between the single and 2x2 array due to the difference in setting up the partial rod structure in CTF.

### 3.1. Single Assembly

The addition of internal bypass, external bypass, and water channels requires the use of unheated conductors in the assembly. It was expected that this would reduce internal assembly coolant temperatures compared to cases without bypass flow because the canister boundaries were no longer adiabatic. Consequently, the pressure may also see small deviations, since the water rod is modeled as a solid adiabatic square rod, the coolant recirculates through the fuel rod leading to a slightly higher pressure drop when compared to the third model with the water rod. However for these models, pressure was used as the outlet boundary condition and therefore should end at the same value. If anything, small variations would be at the lower portions of the axial position. Therefore any small changes are due to liquid sub cooling and recirculation flow. Figure 6 shows very little change between the pressures with each case.

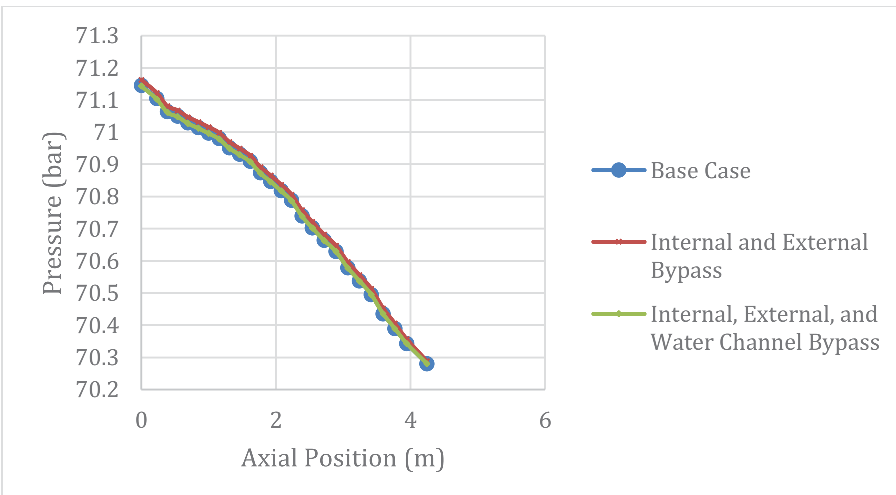


**Figure 6: Pressure over the axial position for single BWR assembly**

The effect of the variation becomes more apparent when graphing the void fraction shown in Figure 7, in which a small difference was seen in the maximum amount of vapor generated and the location at onset of significant void. The inclusion of the bypass theorized that the void vapor faction would be slightly less than that of the model without it. This agrees with the recirculation theory discussed above. Therefore, the location of significant void would be expected to be upstream with the presence of the bypass, since the bypass would allow removal of heat. However note that with the bypass, less coolant would circulate through the fuel rods and thus increase the void generation, which can be seen at the end. However, as shown, the void increases slightly at the end, which was likely due to the mass flow rate being kept constant with each variation. Adding a water channel to the internal/external bypass model has little effect because the internal and external bypass have a larger surface area in contact with the sub-channels when compared to the water channel.

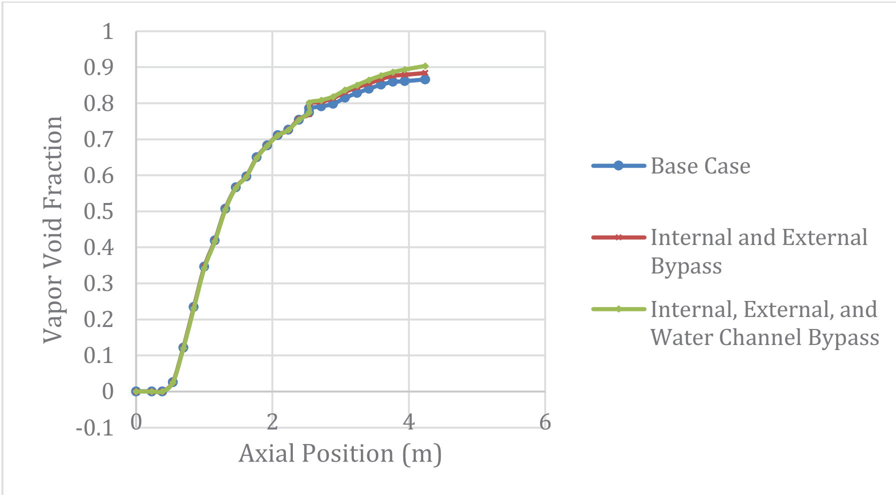


**Figure 7: Vapor Void Fraction over axial position for single BWR assembly**

3.2. 2x2 Assembly

The second model was expected to show similar results to the first model, however note that since this model contains multiple assemblies, internal and external bypasses are simulated. Unheated conductors that are between assemblies are considered internal, while surrounding ones are considered external. This was not expected to change the overall trend. It did change the difference between the variations, specifically the base case and the other two. Looking at Figure 3 the base case was similar to the original model in that it behaves like one very large flow channel since the assemblies do not connect at the bottom and top of the model. The pressure change over the axial position presented in Figure 8 showed similar pressure change over the axial position.

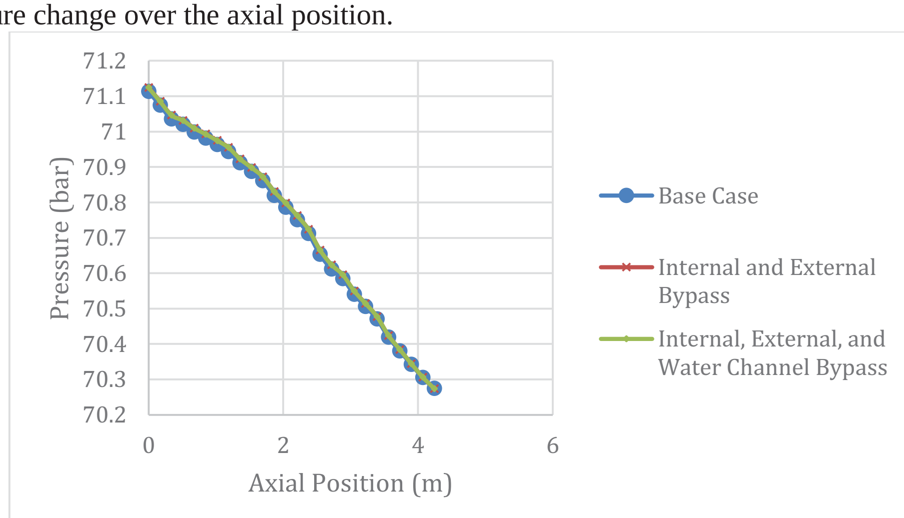


**Figure 8: Pressure over axial position for 2x2 BWR array**

The void fraction drop between variations did not show any substantial change. We see slight differences in the void in Figure 9, but not a discernable amount. The void would be expected to change only slightly like the first model. Therefore, a small change between the models did occur, which will be discussed in the next section. The modeling of the geometry variation in model 2 showed the same trends saw in model one, which lead to the observation that both modeling techniques were verified. Conversely, there was no discernable change between the additions of the water channel in the model 2 results. This could be due to its size compared to the size of the total bypass. One possible reason may deal with the heat conduction between the two. There was also the possibility that the bypass changes the void fraction to the point of maximum and as result any more details will show diminishing returns (water channels in this case). Comparing these results to the full core will conclude whether or not the water channel has a strong effect due to the multiple types of assemblies.

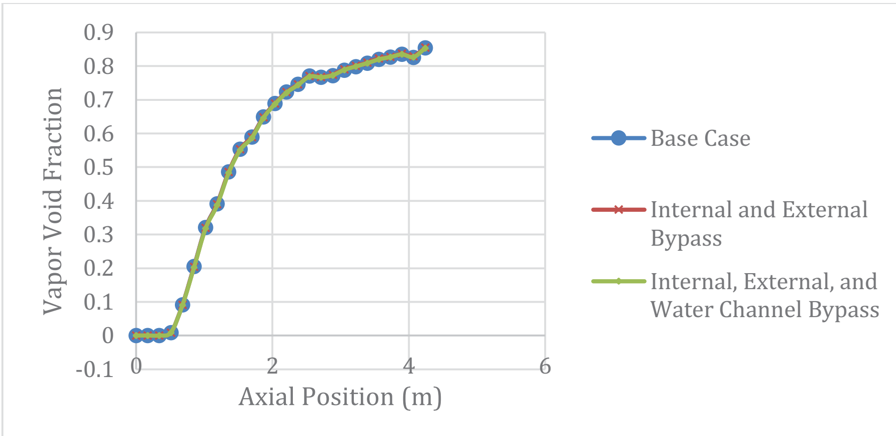


**Figure 9: Vapor void fraction over axial position for 2x2 BWR array**

3.3. Overall Comparisons between Models 1 and 2

The first two models had the same operating parameters, with the only difference being 1 assembly versus 4 assemblies. However the first used split sections within CTF and the second model was created using geometry variation for the partial rods. Even though, it was expected that the pressure and void results be the same. Figure 10 shows the same overall trends. The Pressure showed a slight difference between the variations, but it was close. Theoretically, the values between the two models should have been identical. Similar results were found when graphing the void fraction, however a small difference was expected here due to the removing of heat from additional bypass regions. Therefore a comparison between the pressure in bypass regions and in the bundle region for both models was created and shown in Figure 12. The results should have been identical for each data set, however it was predicted that the models would not match due to reasons discussed above. The pressure in the bypass region for model 1 shows a noticeable difference. This was due to either a difference in the wetted perimeter or the flow rate. If the bypass region has less wetted perimeter (less wall friction), than the bundle average must be lower. The total mass flow rate was kept at 0 for the initial operating conditions of each variation. Also the boundary conditions for the mass flow rate did not change between variations. Realistically, the regions are connected and, therefore, would have the exact same pressure drop. To stabilize the fact that there was less wetted perimeter in the bypass region, the flow velocity would increase in that region, which is what drives the bypass flow rate. Therefore it should theoretically increase too. Since it does not, small changes between the pressure in models one and two were not surprising.

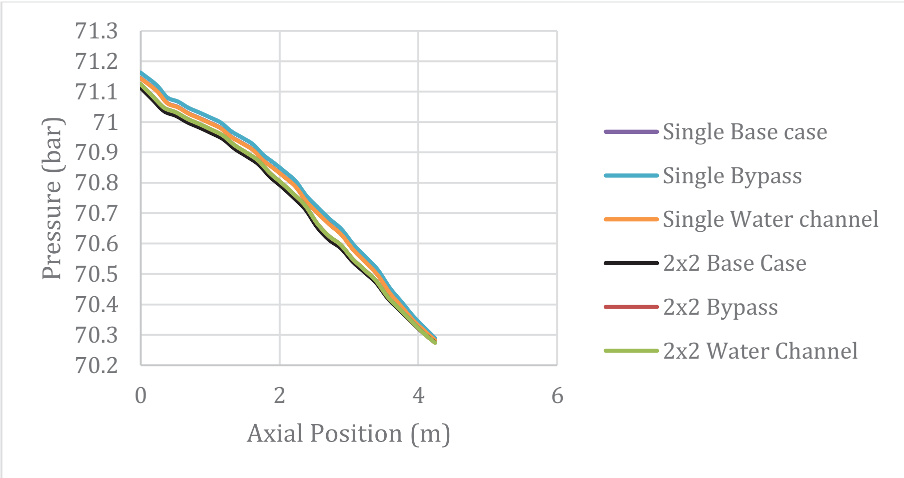


**Figure 10: Pressure over axial pressure for single and 2x2 BWR assembly**

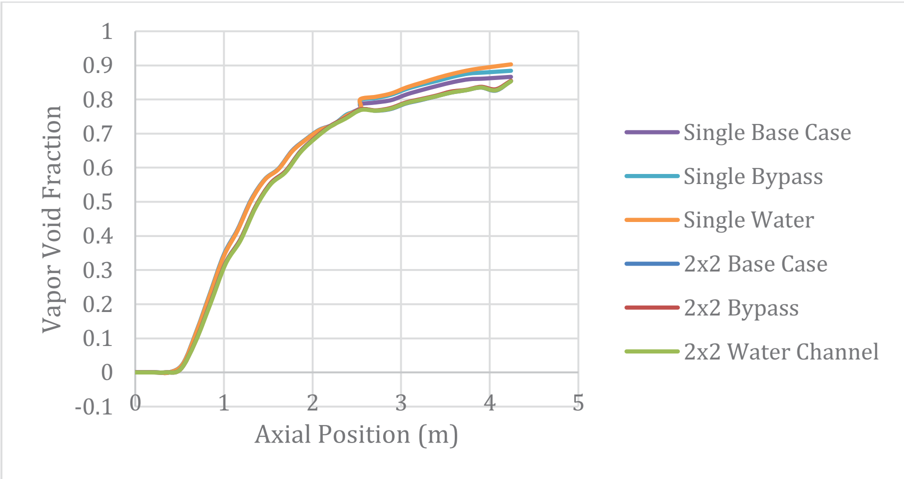


**Figure 11: Vapor void fraction over axial pressure for single and 2x2 BWR assembly**

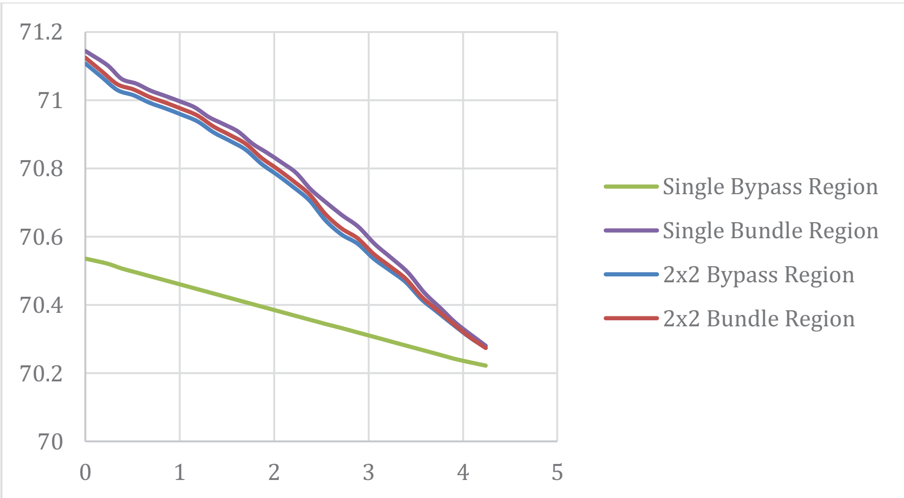


**Figure 12: Pressure over axial position for bundle and bypass regions**

### 3.4. Full Core

The full core model was able to be rebuilt in the systems code TRACE, allowing for further comparison. The TRACE model was originally used with the neutronics code PARCS, therefore minor alterations were made to the model to allow it to be used for single steady state analysis. Note that the data taken from CTF for the axial position goes to the top of the rod, 3.712 m. However the results gathered from TRACE end at the last spacer position in channel 4, 3.3953 m. The model defined the bypass regions in the same format as the full core model, on assembly level.

The full core model showed similar trends to the previous models due to the similar input values. However, note that this was on assembly level and not pin level like the previous models were. Also there were 4 different types of assemblies, and therefore each were analyzed. As said earlier, the four assembly types have different patterns and loss coefficients. Some differences were expected, and some assumptions were added as shown in Table 3. Figure 13-Figure 15: Pressure over axial position for type 1 assemblies below show similar drop in pressure between the variations at low axial levels which converge on the same values as the position increase. It was apparent that the addition of the water channels did have a small effect on the pressure drop. This was most likely due to the multiple assembly types and core configuration. It agreed with the results from the previous tests in that very little actually changed between the two and most likely due to the diminishing returns since the bypass itself caused a noticeable drop in pressure.

The results of each assembly in TRACE are extremely close to each other. This is most likely due to how the systems code works and models the assembly when compared to how a subchannel code like CTF models the assembly. It is shown that a subchannel code will show finer details within the reactor vessel while a systems code is more for overall reactor operations. This is clearly shown here and therefore may be a large indicator why CTF and TRACE behave differently. Also note that TRACE has an abrupt change at around .25 m, which is most likely due to the iterative nature of the code disagreeing with the initial conditions set by the specifications.

When compared to TRACE, the results showed a large discrepancy for all four assembly types. This difference was found to be attributed to the spacer grid loss coefficients associated with the assemblies. Type 2 and 3 assemblies had the highest loss coefficient, while type 1 had the lowest. This directly correlates to how large of a difference CTF and TRACE were in the plots. So it can be seen that having a higher loss coefficient, the pressure drop was greater [12]. According to the TRACE User's Manual, TRACE does not currently allow spacer grids with CHAN components, which are what were used for the model [14].

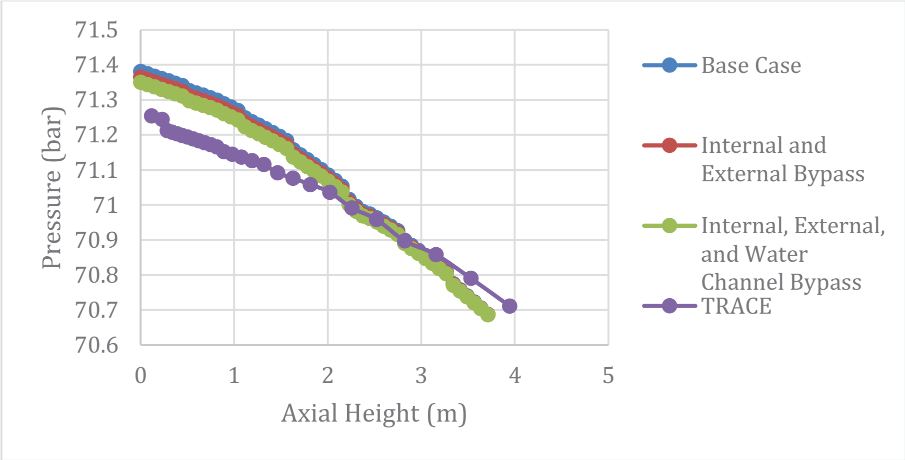


**Figure 13: Pressure over axial position for type 4 assemblies**

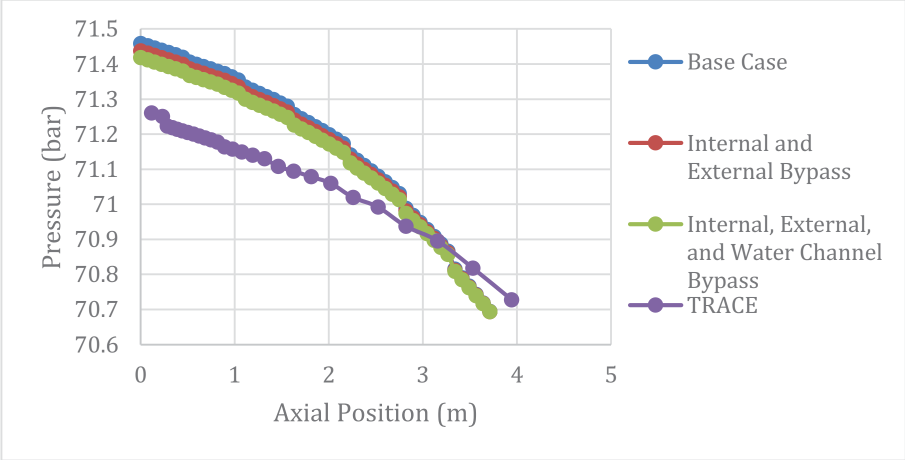


**Figure 14: Pressure over axial position for type 2 and 3 assemblies**

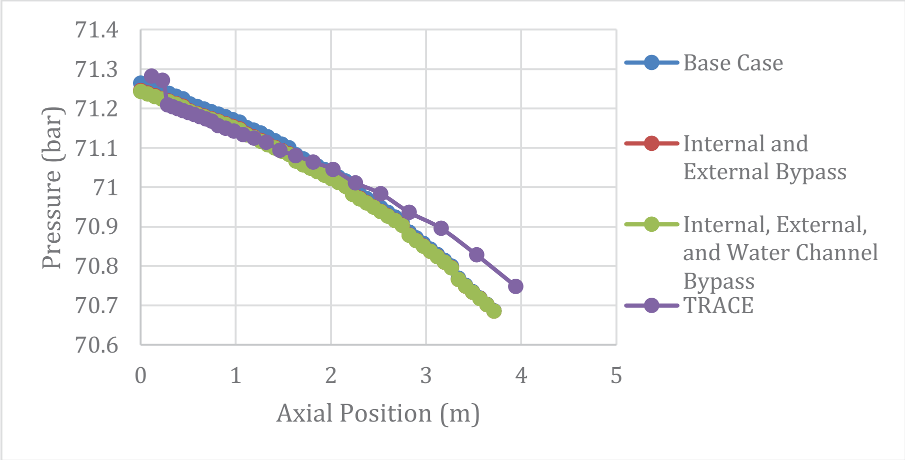


**Figure 15: Pressure over axial position for type 1 assemblies**

The void fraction results were consistent with the other two models and showed similar results. The void fraction changed slightly based on each assembly structure. It was assumed to be the same reason as before being that the addition of the bypass causes a slight change to the void. As a result verifying the usage of pin by pin and assembly levels, since the results are expected to be similar. It was clear that there are small dips present in the void fraction that show up mainly in the full core design (while the other two are unnoticeable). One possible reason was the location of spacer grids were more evident here and caused a slight change in the void fraction due to mixing. Note that spacer grid losses were only listed in bundle channels, no losses were added to internal, external or water channel bypass regions. The mixing will increase heat transfer, but reduce the enthalpy imbalance between the subchannels. As a result there would be an overall reduction in the void fraction until it would travel further down till it reaches the next mixing vanes and repeat. Overall the fluid properties show consistent phenomena expected in BWRs, and it is important to note that on assembly level, the full core BWR shows a small change, but noticeable effect with the addition of water channels.

The TRACE comparison showed similar differences again here that were present with the pressure comparisons. The main reason a difference was shown is likely due to the spacer grids causing a slight change in the amount of void in the system. Another observation was the response to rapid change between the two codes. Looking at Figure 17Figure 18, the TRACE prediction is slightly above CTF's prediction until roughly 1m, which then CTF shows the void fraction increase rapidly, while TRACE shows a more gradual increase. Therefore, this difference in how each code handles rapid change, can greatly affect the overall trend. It is apparent, that both codes predict the same trends, but CTF shows slightly adaptability. However this may be due to the modeling scheme used in TRACE, since it does not support spacer grids at the time.

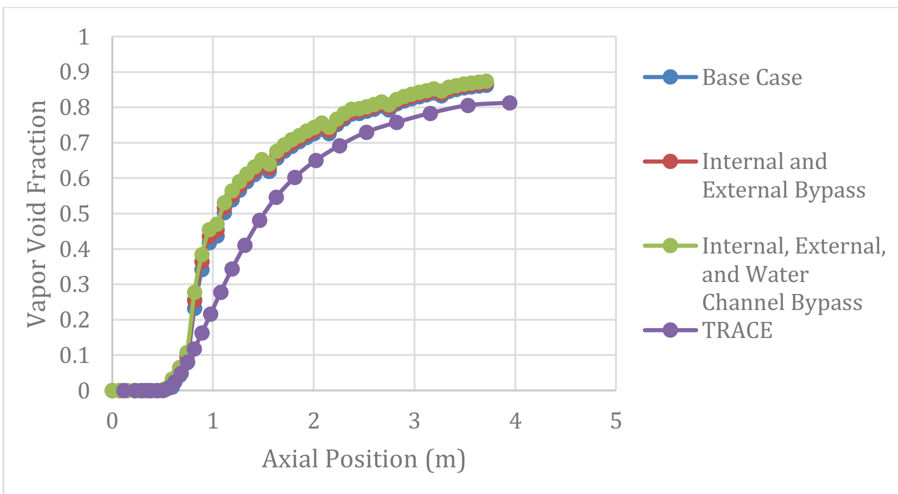


**Figure 16: Vapor void fraction over axial position for type 4 assemblies**

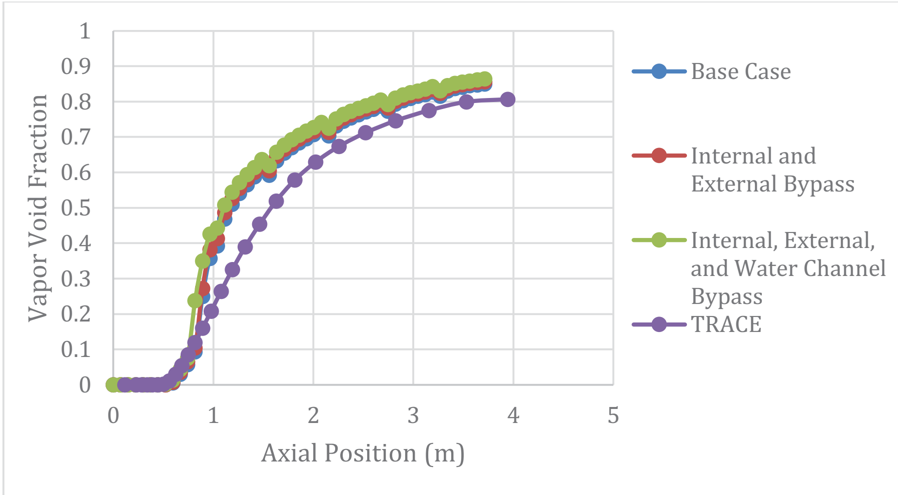


**Figure 17: Vapor void fraction over axial position for type 2 and 3 assemblies**

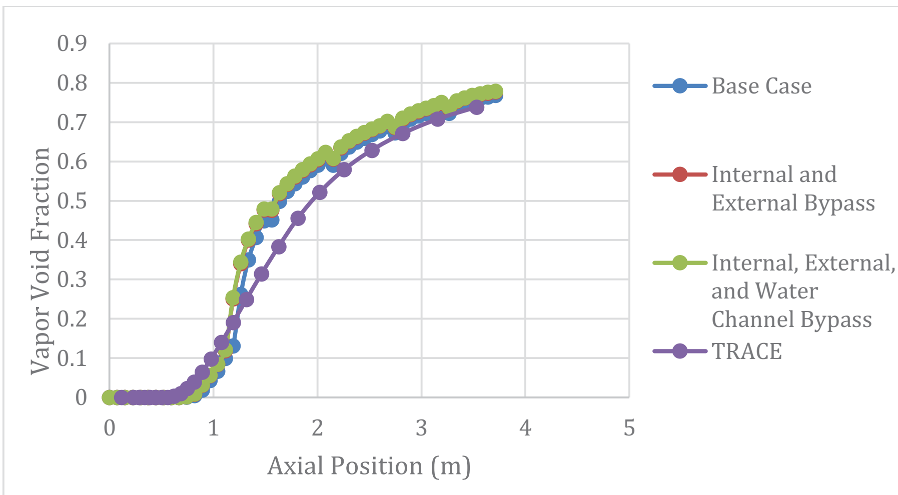


**Figure 18: Vapor void fraction over axial position for type 4 assemblies**

## 4. CONCLUSIONS

The simulations discussed within this paper represent different models of BWRs. The single assembly on pin by pin level represents CTF's capabilities of detailed flow modeling within BWR assemblies. The results demonstrate the effects of adding a bypass and water channel within the model. For the single assembly, a clear difference is shown once the bypass is added. The bypass results demonstrated a clear impact on the overall bundle pressure. The addition of the water channel did not display as strong of a drop. This change is much more dominant in the void fraction, which reduces substantially, which is expected due to the bypasses and water channels acting as unheated conductors. The single assembly model is developed by dividing the CTF input into two sections due to the partial fuel rods being present as in most BWRs. The second model shows strong agreement with the first, and it must be noted that it is modeling using geometry variation inside of splitting the input into two sections. Therefore, CTF is capable of modeling common BWR geometry in multiple ways allowing for more diversity. The results shown are for bundle average fluid properties and therefore, the effects of the water channel are not as clear as the bypass, since the size of the bypass (internal and external) are much larger than that of the water channel. The full core analysis showed similar results as the previous models, however the water channels do show a slight change here. One important comparison is looking at the outer assemblies versus the inner ones where the external bypass not affect them as much. Overall CTF models key fluid property parameters very well and shows the changes when additional detail is added.

The results from CTF simulations of the Oskarshamn-2 benchmark specifications show strong representation of fluid properties in current BWR models. The pervious CTF simulations and validations show its versatility and strength in modeling BWRs.

**ACKNOWLEDGMENTS**
This work was performed within a cooperation between PSU and CASL.

**REFERENCES**

1. M. J. Thurgood et al., “COBRA-TF Development,” Proc. Of 8th Water Reactor Safety Information Meeting. 1980
2. M. Avramova, D. Cuervo, K. Ivanov, "Improvements and Applications of COBRA-TF for Stand-Alone and Coupled LWR Safety Analyses", Proceedings: PHYSOR-2006, Vancouver, Canada, September 2006
3. D. Todd, C. Frepoli, L.E. Hochreiter, “Development of a COBRA-TF Model For The Penn State University- Rod Bundle Heat Transfer Program’, ICONE – 1999, Tokyo, Japan, April 1999
4. M. Gluck, “Validation of the sub-channel code F-COBRA-TF: Part I. Recalculation of single-phase and two-phase pressure loss measurements”, Nucl. Eng. Des., 238(9) 2008, pp. 2308-2316.
5. M. Avramova, “COBRA-TF development, qualification, and application to light water reactor analysis”, MS Thesis, The Pennsylvania State University, 2003
6. G.B. Wallis. One-Dimensional two-phase flow. McGraw-Hill, 1969
7. J. Magedanz, Y. Perin. M. Avramova, A. Pautz, “ High-Fidelity Multiphysics Simulation of BWR Assembly With Coupled TORT-TD/CTF” *Proceedings of PHYSOR Conference,* Knoxville, Tennessee, U.S.A. April 15-20, 2012
8. C.Y. Park, L.E. Hochreiter, J.M. Kelly, and Kohvt, R.J., “Analysis of FLETCH-SEASET 163 Rod Blocked Bundle Data using COBRA-TF’, NUREG-CR-4166, JANUARY 1986.
9. M. Avramova, et al., “Analysis of Void Distribution Predictions for Phase I of the OECD/NRC Benchmark using CTF/NEM”, Proceedings: NURETH-12, Pittsburgh, Pennsylania, USA, September 2007
10. M. Avramova, et al., “Assessment of CTF Boiling Transition and Cirtical Heat Flux Modeling Capabilities Using the OECD/NRC BFBT and PSBT Benchmark Databases”, Proceedings: NURETH-14, Toronto, Ontario, Canada, September 2011
11. Jimenez E, Javier, and Y. Perin. Description of the CTF Input for BWR ATWS Analysis. Rep. no. D13.22. N.p.: NURESAFE, n.d. Print.
12. C. Keckler, T. Kozlowski, M. Avramova, K. Ivanov, “Comparisons of Thermal-Hydraulic Modeling with CTF and TRACE using the Oskarshamn-2 Benchmark” The Pennsylvania State University, 2014
13. M. Avramova, R. Salko. CTF Theory Manual. Vol. 1. Pennsylvania: Reactor Dynamics and Fuel Management Group, n.d. Print.